

## Construction of Autonomic Self-Healing $\text{CO}_2$ -Based Polycarbonates via One-Pot Tandem Synthetic Strategy

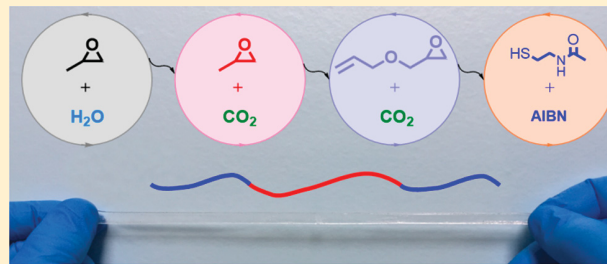
Guan-Wen Yang,<sup>†</sup> Yao-Yao Zhang,<sup>†</sup> Yanyan Wang,<sup>‡</sup> Guang-Peng Wu,<sup>\*,†,ID</sup> Zhi-Kang Xu,<sup>†,ID</sup> and Donald J. Darensbourg<sup>\*,‡,ID</sup>

<sup>†</sup>MOE Laboratory of Macromolecular Synthesis and Functionalization, Adsorption and Separation Materials and Technologies of Zhejiang Province, Department of Polymer Science and Engineering, Zhejiang University, Hangzhou 310027, China

<sup>‡</sup>Department of Chemistry, Texas A&M University, 3255 TAMU, College Station, Texas 77843, United States

### Supporting Information

**ABSTRACT:** The coupling of epoxides and carbon dioxide to polycarbonates ( $\text{CO}_2$ -PCs) has been the subject of intense research for nearly half a century. Although tremendous progress has been achieved, their aliphatic characteristics and lack of functionalities of  $\text{CO}_2$ -PCs limit the scope of their application in high value-added and functional materials. In this article, the first  $\text{CO}_2$ -based polycarbonate with the ability to autonomously self-heal is constructed via a one-pot synthetic strategy. The key to the success of the synthetic strategy is efficient tandem three different catalytic reactions, i.e., hydrolysis of epoxides, immortal copolymerization of  $\text{CO}_2$ /epoxides, and thiol–ene click reactions in a one-pot process. Based on the standard tensile testing, these  $\text{CO}_2$ -based materials show robust self-healing properties, where the extensibility, maximal strength, and Young's modulus of the specimens can almost entirely recover to their original value under ambient temperature. Our studies demonstrate that the self-healing capability of these  $\text{CO}_2$ -based materials arises both from the *homo*-hydrogen bonding (between amide groups) and the *hetero*-hydrogen bonding (between amide group and carbonate group of polycarbonate backbone). The convenient and atom economic synthesis strategy, combined with the impressive self-healing capability for these materials, should expand the library of high value-added  $\text{CO}_2$ -based polycarbonates and the scope of their applications.



## INTRODUCTION

Beginning with Inoue's discovery in 1969, the catalytic coupling of epoxides and carbon dioxide to polycarbonates ( $\text{CO}_2$ -PCs) has been the subject of intense research for nearly half a century.<sup>1</sup> The driving force for this catalytic transformation is the use of  $\text{CO}_2$ , a nontoxic, abundant, and cheap C1 source, to produce a wide variety of degradable polycarbonates. This transformation provides in many instances an attractive alternative route to the current polycarbonate production technology which is based on the polycondensation of diols and phosgene or phosgene derivatives.<sup>2</sup> Under a global concerted effort, enormous progress has been achieved for this transformation, particularly utilizing well-defined hetero- and homogeneous catalyst systems.<sup>3–9</sup> Based on these systems,  $\text{CO}_2$ -PCs with controlled molecular weights, ether linkages suppression, thermoresistance, regio- or/and stereoselectivity, and crystalline property have been well-developed.<sup>10–18</sup> Regardless of such advances, current attempts at the industrialization of this transformation are limited to propylene oxide (PO) and ethylene oxide (EO) and its derivatives to produce poly(propylene carbonate) (PPC), poly(ethylene carbonate) (PEC), and their analogues.<sup>19</sup> The most important industrial interest in  $\text{CO}_2$ -PCs stems from the motivation that the production of PPC and PEC polyols can be used in

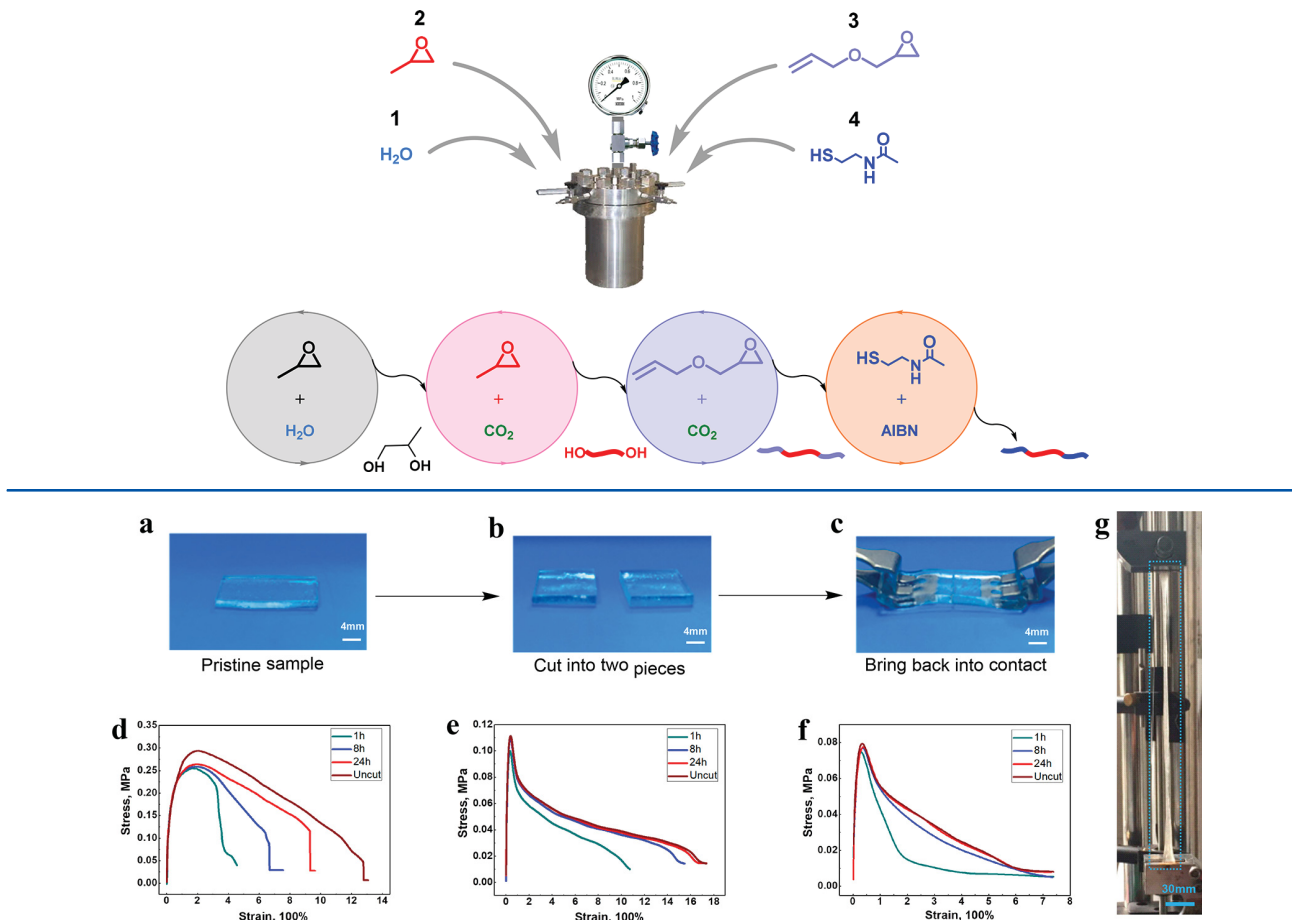
condensation reactions with diisocyanates to afford one of the most widely used polymers in modern society, polyurethane.<sup>20</sup> This limited scope of the application for  $\text{CO}_2$ -PCs could be attributed to their aliphatic characteristics and lack of functionalities, preventing their use in high value-added and functional materials. Therefore, the synthesis of more diverse  $\text{CO}_2$ -PCs with different functionalities is highly needed to meet the demands of various applications.

During the past decade, self-healing materials have sparked great interest in polymer chemistry due to their great potential to deliver products with improved durability, extended lifetime, and maintained structural integrity.<sup>21–29</sup> To date, many types of self-healing materials via encapsulation of healing agents,<sup>30</sup> employment of thermally irreversible and reversible covalent bonds,<sup>31–36</sup> and supramolecular assemblies<sup>37,38</sup> have been well developed. Among various self-healing materials being investigated, autonomic healing polymers based on H-bonding are more desirable due to their mild processing conditions and reversibility as well as no need for an external stimulus.<sup>39–41</sup> Recently, we have been particularly interested in designing

Received: December 21, 2017

Revised: February 1, 2018

Published: February 9, 2018

Scheme 1. Strategy Performed for Preparation CO<sub>2</sub>-Based Self-Healing Materials

**Figure 1.** Photographic sequences of sample specimens tests and the corresponding self-healing results: (a) a pristine sample, (b) the sample was cut in half, and (c) the two halves were then gently brought back into contact for 1 min. The mechanical and self-healing properties of the three samples: (d) P1, (e) P2, and (f) P3. (g) A screenshot for a P2 specimen (in dashed rectangle) subjected to the standard stress-strain tensile test, after spontaneously self-healing for 24 h under ambient conditions without any external stimulus.

functional CO<sub>2</sub>-PCs to expand their applications, particularly by the development of CO<sub>2</sub>-based copolymers to introduce diverse functionalities. These CO<sub>2</sub>-based copolymers have shown great potential for biomedical purposes, nanodevices, and lithography.<sup>42–47</sup> Encouraged by our studies on construction of CO<sub>2</sub>-based block polymers and the understandings on the self-healing materials design, herein, the first example of CO<sub>2</sub>-based polycarbonate with autonomic self-healing capability is reported (Scheme 1). A noteworthy feature of our report is that the self-healing CO<sub>2</sub>-PC materials could be conveniently constructed in a one-pot strategy by tandem three different chemical reactions including hydrolysis of epoxides, immortal copolymerization of CO<sub>2</sub>/epoxides, and thiol–ene click reactions. Using the tandem strategy, CO<sub>2</sub>-based block copolymers with different ratios of stiff and soft domains are easily synthesized and systematically studied. In the materials, the stiff polycarbonate domain provides mechanical strength and the soft part allows for the self-healing capacity. Based on the standard stress–strain tensile test, our CO<sub>2</sub>-based materials display favorable mechanical performance and robust self-healing properties, where the extensibility, maximal strength, and Young's modulus of the materials can almost entirely recover their original values without any external stimulation under ambient temperature.

## RESULTS AND DISCUSSION

Our synthesis strategy for the preparation of CO<sub>2</sub>-based self-healing materials is illustrated in Scheme 1, and more details are provided in Figure S1 of the Supporting Information. A certain amount of water was intentionally added to the PO/CO<sub>2</sub> copolymerization process with the salenCoTFA/PPNTFA catalytic system (Figure S2). Given the high speed of the hydrolysis of PO in the presence of the cobalt complex, PO reacts with the added water first to generate the corresponding 1,2-propanediol, which worked as a chain transfer agent during the following copolymerization of PO and CO<sub>2</sub>, giving the corresponding  $\alpha,\omega$ -dihydroxy end-capped PPC (HO-PPC-OH). It should be parenthetically noted here that the formation of high-quality HO-PPC-OH benefited from the trifluoroacetate initiating group, which has been investigated and proven to undergo hydrolysis rapidly and easily during the epoxide/CO<sub>2</sub> copolymerization in our and others' studies.<sup>45,48,49</sup> After full conversion of PO, the unreacted CO<sub>2</sub> was released, and a precalculated amount of allyl glycidyl ether (AGE), a popular monomer for incorporating functional groups via its double bond,<sup>44,50–55</sup> was added to the reactor. After recharging the reactor with CO<sub>2</sub>, the generated HO-PPC-OH served as a macro-chain-transfer agent to incorporate the AGE/CO<sub>2</sub>

Table 1. Characterization and Mechanical and Self-Healing Properties of P1–P3

polymer	PPC/PACC <sup>a</sup> (mole ratio)	$M_n^b$ (kg/mol)	$M_w/M_n$	$T_g^c$ (°C)	mechanical properties			self-healing (% recovery of extensibility)		
					$E^d$ (MPa)	$\sigma^e$ (MPa)	$\epsilon^f$ (%)	1 h	8 h	24 h
P1	3:2	17.8	1.05	0.3; 40	1.8 ± 0.05	0.3 ± 0.01	1300 ± 40	36 ± 1	52 ± 2	73 ± 2
P2	1:1	19.0	1.03	-0.1; 31	0.9 ± 0.03	0.12 ± 0.005	1700 ± 50	61 ± 2	89 ± 2	99 ± 1
P3	2:3	21.1	1.03	0.2; 19	0.6 ± 0.02	0.08 ± 0.004	750 ± 20	99 ± 1	99 ± 1	99 ± 1

<sup>a</sup>Determined by <sup>1</sup>H NMR spectroscopy. <sup>b</sup>Determined by GPC using polystyrene standards in THF. <sup>c</sup>Determined by DSC. <sup>d</sup>Young's modulus, taken as the slope of the initial part of the stress–strain curve. <sup>e</sup>Maximal strength, taken at the maximal point along the stress–strain curves. <sup>f</sup>Strain at break, strain rate = 100 mm/min, 25 °C. All mechanical properties were determined from three replicates for each sample.

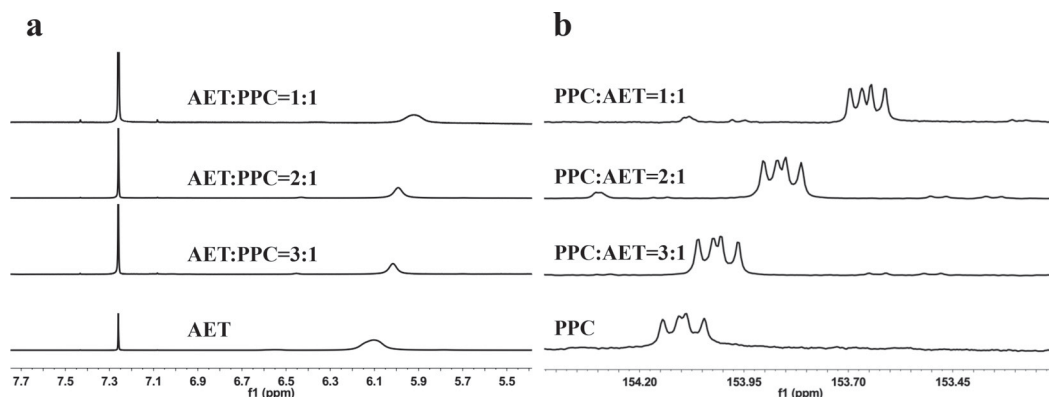
copolymer blocks, affording the corresponding PPC/poly(allylglycidyl ether carbonate) (PAC) triblock copolymers. The polymerization was continued for sufficient time to ensure complete conversion of AGE. Following careful release of CO<sub>2</sub>, the radical-mediated thiol–ene click reaction was achieved by the addition of 2-(acetylaminio)ethanethiol (AET). After complete conversion, our objective CO<sub>2</sub>-based block copolymers were obtained in quantitative yield. For simplicity, the objective block copolymer is referred to as PACC-*b*-PPC-*b*-PACC in the ensuing paragraphs.

The specific NMR signal assignments (Figures S3–S5) coupled with predictable molecular weight and unimodal distribution on GPC curves of the obtained polymers (Figure S6) indicate the success of our tandem strategy. The corresponding intermediate in each synthesis step was also characterized by GPC and <sup>1</sup>H NMR, and the detailed synthesis procedure and characterization are provided in the Supporting Information. Two glass transition temperatures at ~0 °C for the PACC block and 19–40 °C for the PPC block indicated the occurrence of microphase separation for the materials as characterized by differential scanning calorimetry (DSC) (Figures S7–S9). In order to systematically study the material performance, three PACC-*b*-PPC-*b*-PACCs with different PPC/PACC mole ratios were synthesized and were abbreviated as P1 (PPC/PACC = 3/2), P2 (PPC/PACC = 1/1), and P3 (PPC/PACC = 2/3).

Before evaluation of the self-healing properties of the obtained materials, the mechanical performance was initially characterized via static uniaxial tensile testing. Standard specimens for tensile testing (20 × 8 × 2 mm) were hot-pressed at a plate vulcanizing machine under 120 °C and 10 MPa for 8 min. The stress–strain curves of P1–P3 are plotted in Figure 1, and their key mechanical properties are summarized in Table 1. Based on the tensile testing, the stiffness and strength of the materials decrease with the increasing of the PACC blocks because of the relative low  $T_g$  of PACC. The P1 with 40 mol % of PACC has a Young's modulus (calculated by the slope of the initial part of the stress–strain curve, Figure 1) of ~1.8 MPa, maximal strength of ~0.3 MPa, and strain-at-break of ~1300%. When the mass ratio of PACC domain increased to 60 mol % for P3, the  $T_g$ 's of the PPC block and the PACC blocks both are lower than ambient temperature. The material behaves like a viscous substance and has the weakest Young's modulus (~0.6 MPa), maximal strength (~0.08 MPa), and the lowest elongation (~750%) of all three samples. When the PACC block is around 50 mol %, a Young's modulus of ~0.9 MPa, maximal strength of ~0.12 MPa, and the highest strain-at-break of ~1700% were observed for P2, presumably due to the good balance of hard PPC and soft PACC domains.

Based on the mechanical properties testing, the autonomic self-healing behavior of these materials was then examined at room temperature. Self-healing tests were conducted by cutting sample specimens into two completely separate pieces by a sharp blade, and then the two pieces were contacted gently to ensure the cut surfaces fit entirely for 1 min. The two faces spontaneously self-heal over time under ambient conditions (Figure 1a–c). After healing for a certain period of time, the sample specimens were subjected to a standard stress–strain tensile test at the pulling rate of 100 mm/min. The tensile test for the pristine samples and self-healing samples are shown in Figure 1d–f, and the results are summarized in Table 1. As shown in Figure 1, the healing properties were time-dependent. Increasing the healing time generally leads to better recovery of both tensile strength and extensibility of the sample specimens. All the healing specimens are able to regain their Young's modulus (initial stiffness) as indicated by the good overlap of the initial region of stress–strain curves between the healed and pristine samples. After healing 1 h, the extensibility of P1, P2, and P3 recovered ~36%, ~61%, and ~100%, respectively. Meanwhile, the maximal strength recovered ~86%, ~89%, and ~93%, respectively. After healing 24 h, P1 recovered ~73% of extensibility and ~90% of maximal strength. To our gratification, the P2 and P3 nearly completely recovered their extensibility and maximal strength, as the stress–strain curves of healing samples of P2 and P3 were almost entirely overlapping the curve of their pristine samples after healing 24 h. Figure 1g is a screenshot for a healing P2 specimen (in dashed rectangle) subjected to the stress–strain tensile test after spontaneously self-healing for 24 h, where a strain-at-break of over 1700% (approximately equal to the pristine sample) was observed, demonstrating the great healing capability of our designed CO<sub>2</sub>-based polymers.

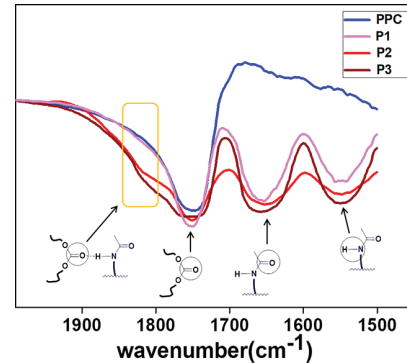
With the impressive healing capability of block copolymers in hand, our interest focused on the self-healing mechanism, since an understanding of the chemistry and physics of macromolecules is a prerequisite for the development and application of new materials. First, in order to verify that the self-healing property for these materials relies on the employment of reversible H-bonding, we investigated the self-healing behavior of the samples at different humidity environment since water should be able to destroy the hydrogen bonds of the polymer chains and thus influence the self-healing ability of the materials. The tensile results of these samples after healing 24 h are shown in Figure S10, and it is obvious that higher humidity environment results in reduced mechanical property recovery. In addition, water works as a plasticizer; thus, the plasticizing effect of H<sub>2</sub>O to the PACC phase should also be considered. As a result, the reduced mechanical recovery property can be attributed to new hydrogen bond formation



**Figure 2.** (a) <sup>1</sup>H NMR signals of amide group of AET with different contents of PPC and (b) the accompanying <sup>13</sup>C NMR signals carbonyl group of PPC (conditions: the mole ratio of the carbonate unit of PPC to amide group of AET = 3/1, 2/1, and 1/3, in CDCl<sub>3</sub>).

between water molecules and the amides group on the freshly cut surface, thus reducing the mobile PACC soft domains cross the fracture interface when the surfaces are brought back into contact.

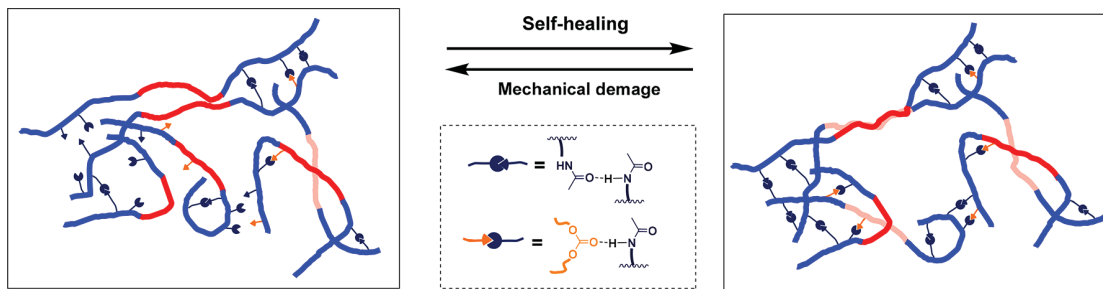
The above experiment revealed that the self-healing property for these materials relies on the employment of the reversible H-bonding; however, we suspect that the hydrogen bonding interaction not only occurred between the amides (—NH—CO— to —NH—CO— groups, *homo*-hydrogen bonding) but also existed between the carbonate groups on polycarbonate backbones and the amide groups (—O—CO—O— to —NH—CO—, *hetero*-hydrogen bonding) in our materials since there are abundant carbonate groups on the polycarbonate backbones. In order to verify our speculation, solutions with different ratios of PPC homopolymers to AET small molecules were characterized by NMR measurements (Figure 2). To avoid the solvent effect, the experiment was performed in CDCl<sub>3</sub>, a nonpolar solvent. Figure 2a shows the change of the chemical shift of the amide group of AET with different amounts of PPC homopolymers. The proton of the amide was located at 6.10 ppm in neat CDCl<sub>3</sub>. Upon the addition of PPC homopolymers, the proton peak of amide group gradually shifts to higher field (from 6.10 to 5.92 ppm). Meanwhile, the variation of the carbonate unit of PPC was also monitored by <sup>13</sup>C NMR. As indicated in Figure 2b, the carbonyl peak of PPC gradually shifts to higher field (from 154.10 to 153.67 ppm) with increasing amount of AET. Furthermore, the <sup>13</sup>C NMR measurement of the block polymers was also performed, and the carbonyl peak of carbonate unit also shifts to a slightly higher field with increasing amount of PACC block (Figure S11). These results indicate the generation of *hetero*-hydrogen bonding interaction between the carbonate groups of polycarbonate backbones and the amide groups in our materials. Furthermore, FT-IR spectroscopy was also performed to evaluate the formation of *hetero*-hydrogen bonding in bulk samples. As shown in Figure 3, a shoulder at around 1815 cm<sup>-1</sup> (the C=O stretching peak of carbonate units at 1750 cm<sup>-1</sup>), characteristic of the formation of *hetero*-hydrogen bonding, was clearly observed with increasing of PACC domain. In addition to these expected changes in IR signals, the signal at ~1655 cm<sup>-1</sup> (amide groups) broadened with the increasing amount of the PACC block, which leads us to conclude the formation of *hetero*-hydrogen bonding between polycarbonate backbones to the amide groups.



**Figure 3.** FT-IR spectroscopy of pure PPC and P1–P3 samples. The signals at 1750 and 1655 cm<sup>-1</sup> are the absorbances of the carbonyl and amide groups, respectively.

Based on the aforementioned understanding, the self-healing mechanism is proposed in Scheme 2. In our materials, because of the relatively high  $T_g$ , the PPC phase constrains the chain motion and works as the stiff domain to keep the mechanical strength, while the soft PACC phase provides H-bonds for the self-healing agent. Meanwhile, the phase separation between the PPC block and the PACC blocks leads to the hard PPC polymer chains aggregating together, providing physical cross-links in the materials. When the two damaged faces are contacted, rearrangement of the mobile soft domains is stimulated across the fracture interface, and the *homo*-hydrogen bonds (between amide groups) and *hetero*-hydrogen bonds (between amide group and carbonate group) are regenerated. It should be noted that the *homo*- and *hetero*-hydrogen bonds generated exist both inter- and intrablock copolymers (Scheme 2), leading to excellent autonomic self-healing capability.

In addition, these designed CO<sub>2</sub>-based materials also show high transparency (Figure S12) and stability. Importantly, there are no chemical changes in the materials during thermoforming process as indicated by <sup>1</sup>H NMR (Figure S13). The small pieces of test specimens could be melt pressed and re-form to bulk materials for reuse, and the thermoforming process could be repeated several times, without any loss in the mechanical and self-healing properties, thus showing profound implications in the future developments of degradable materials.

Scheme 2. Schematic Illustration of the Self-Healing Mechanism of the CO<sub>2</sub>-Based Block Copolymers

## CONCLUSION

In summary, the first CO<sub>2</sub>-based autonomic self-healing polycarbonates were synthesized efficiently in a one-pot strategy. The synthetic strategy is enabled by the judicious choice of tandem three different chemical reactions, including hydrolysis of epoxides, immortal copolymerization of CO<sub>2</sub>/epoxides, and thiol–ene click chemistry. Using this strategy, CO<sub>2</sub>-based block copolymers with impressive self-healing capability were well synthesized and systematically studied. The standard stress–strain tensile test indicates that the extensibility, maximal strength, and Young's modulus of the materials can almost entirely recover after healing for a certain time under ambient temperature, without any external stimulation. Furthermore, we verified that the *homo*- and *hetero*-hydrogen bonding interactions both lead to the remarkably healing capability. The facile synthesis and robust self-healing capacity of these materials should enable future studies in the development of advanced CO<sub>2</sub>-based polycarbonates with new applications. Such investigations are currently underway in our laboratories.

## EXPERIMENTAL SECTION

For information regarding experimental procedures, materials, and other details, see the *Supporting Information*.

## ASSOCIATED CONTENT

### Supporting Information

The Supporting Information is available free of charge on the ACS Publications website at DOI: [10.1021/acs.macromol.7b02715](https://doi.org/10.1021/acs.macromol.7b02715).

Information for experiments and characterization of polymers ([PDF](#))

## AUTHOR INFORMATION

### Corresponding Authors

\*E-mail: [gwpwu@zju.edu.cn](mailto:gwpwu@zju.edu.cn) (G.-P.W.).

\*E-mail: [djdarens@chem.tamu.edu](mailto:djdarens@chem.tamu.edu) (D.J.D.).

### ORCID

Guang-Peng Wu: [0000-0001-8935-964X](https://orcid.org/0000-0001-8935-964X)

Zhi-Kang Xu: [0000-0002-2261-7162](https://orcid.org/0000-0002-2261-7162)

Donald J. Daresbourg: [0000-0001-9285-4895](https://orcid.org/0000-0001-9285-4895)

### Notes

The authors declare no competing financial interest.

## ACKNOWLEDGMENTS

Financial support is acknowledged to Qianjiang Talent-D Foundation (QJD1702025), National Natural Science Foundation of China (Grant 21674090), the National Science

Foundation (CHE-1665258), and the Robert A. Welch Foundation (A-0923) in the USA. G.-P.W. gratefully acknowledges the support of Fundamental Research Funds for the Central Universities and the “Hundred Talents Program” of Zhejiang University from China. The authors thank Prof. Yihu Song and Dr. Xinxin Xia in Zhejiang University for their assistance in tensile test.

## REFERENCES

- Inoue, S.; Koinuma, H.; Tsuruta, T. Copolymerization of carbon dioxide and epoxide. *J. Polym. Sci., Part B: Polym. Lett.* **1969**, *7*, 287–292.
- Bottenbruck, L. *Engineering Thermoplastics: Polycarbonates, Polyacetals, Polyesters, Cellulose Esters*; Hanser Publishers: New York, 1996; p 112.
- Darensbourg, D. J.; Holtcamp, M. W. Catalysts for the reactions of epoxides and carbon dioxide. *Coord. Chem. Rev.* **1996**, *153*, 155–174.
- Coates, G. W.; Moore, D. R. Discrete metal-based catalysts for the copolymerization of CO<sub>2</sub> and epoxides: discovery, reactivity, optimization, and mechanism. *Angew. Chem., Int. Ed.* **2004**, *43*, 6618–6639.
- Darensbourg, D. J.; Mackiewicz, R. M.; Phelps, A. L.; Billodeaux, D. R. Copolymerization of CO<sub>2</sub> and epoxides catalyzed by metal salen complexes. *Acc. Chem. Res.* **2004**, *37*, 836–844.
- Chisholm, M. H.; Zhou, Z. New generation polymers: the role of metal alkoxides as catalysts in the production of polyoxogenates. *J. Mater. Chem.* **2004**, *14*, 3081–3092.
- Darensbourg, D. J. Making plastics from carbon dioxide: salen metal complexes as catalysts for the production of polycarbonates from epoxides and CO<sub>2</sub>. *Chem. Rev.* **2007**, *107*, 2388–2410.
- Kember, M. R.; Buchard, A.; Williams, C. K. Catalysts for CO<sub>2</sub>/epoxide copolymerization. *Chem. Commun.* **2011**, *47*, 141–163.
- Lu, X.-B.; Darensbourg, D. J. Cobalt catalysts for the coupling of CO<sub>2</sub> and epoxides to provide polycarbonates and cyclic carbonates. *Chem. Soc. Rev.* **2012**, *41*, 1462–1484.
- Sugimoto, H.; Inoue, S. Copolymerization of carbon dioxide and epoxide. *J. Polym. Sci., Part A: Polym. Chem.* **2004**, *42*, 5561–5573.
- Luinstra, G. A. Poly(propylene carbonate), old copolymers of propylene oxide and carbon dioxide with new interests: catalysis and material properties. *Polym. Rev.* **2008**, *48*, 192–219.
- Qin, Y.; Wang, X. Carbon dioxide-based copolymers: environmental benefits of PPC, an industrially viable catalyst. *Biotechnol. J.* **2010**, *5*, 1164–1180.
- Klaus, S.; Lehenmeier, M. W.; Anderson, C. E.; Rieger, B. Recent advances in CO<sub>2</sub>/epoxide copolymerization—New strategies and cooperative mechanisms. *Coord. Chem. Rev.* **2011**, *255*, 1460–1479.
- Darensbourg, D. J.; Wilson, S. J. What's new with CO<sub>2</sub>? Recent advances in its copolymerization with oxiranes. *Green Chem.* **2012**, *14*, 2665–2671.
- Lu, X.-B.; Ren, W.-M.; Wu, G.-P. CO<sub>2</sub> copolymers from epoxides: Catalyst activity, product selectivity, and stereochemistry control. *Acc. Chem. Res.* **2012**, *45*, 1721–1735.

(16) Paul, S.; Zhu, Y.; Romain, C.; Brooks, R.; Saini, P. K.; Williams, C. K. Ring-opening copolymerization (ROCOP): synthesis and properties of polyesters and polycarbonates. *Chem. Commun.* **2015**, *51*, 6459–6479.

(17) Lu, X.-B. Stereoregular  $\text{CO}_2$  copolymer: from amorphous to crystalline materials. *Acta Polym. Sin.* **2016**, *9*, 1166–1178.

(18) Poland, S. J.; Daresbourg, D. J. A quest for polycarbonates provided via sustainable epoxide/ $\text{CO}_2$  copolymerization processes. *Green Chem.* **2017**, *19*, 4990–5011.

(19) Presently, attempts at industrialization of  $\text{CO}_2$ /epoxide derived copolymer are mainly concentrated on ethylene oxide and propylene oxide to produce poly(ethylene carbonate) and poly(propylene carbonate) by Blue Chemical, Henan Tianguan, and Tai-zhou Bangfeng in China, SK in Korea, Bayer and BASF in Germany, and Novomer and Empower Materials in the United States.

(20) Langanke, J.; Wolf, A.; Hofmann, J.; Böhm, K.; Subhani, M. A.; Müller, T. E.; Leitner, W.; Gütler, C. Carbon dioxide ( $\text{CO}_2$ ) as sustainable feedstock for polyurethane production. *Green Chem.* **2014**, *16*, 1865–1870.

(21) Yang, J. Y.; Urban, M. W. Self-healing polymeric materials. *Chem. Soc. Rev.* **2013**, *42*, 7446–7467.

(22) de Espinosa, L. M.; Fiore, G. L.; Weder, C.; Johan Foster, E.; Simon, Y. C. Healable supramolecular polymer solids. *Prog. Polym. Sci.* **2015**, *49*–50, 60–78.

(23) An, S. Y.; Arunbabu, D.; Noh, S. M.; Song, Y. K.; Oh, J. K. Recent strategies to develop self-healable crosslinked polymeric networks. *Chem. Commun.* **2015**, *51*, 13058–13070.

(24) Wu, D. Y.; Meure, S.; Solomon, D. Self-healing polymeric materials: A review of recent developments. *Prog. Polym. Sci.* **2008**, *33*, 479–522.

(25) Urban, M. W. Stratification, stimuli-responsiveness, self-healing, and signaling in polymer networks. *Prog. Polym. Sci.* **2009**, *34*, 679–687.

(26) Hillewaere, X. K. D.; Du Prez, F. E. Fifteen chemistries for autonomous external self-healing polymers and composites. *Prog. Polym. Sci.* **2015**, *49*–50, 121–153.

(27) Liu, Y.-L.; Chuo, T.-W. Self-healing polymers based on thermally reversible Diels–Alder chemistry. *Polym. Chem.* **2013**, *4*, 2194–2250.

(28) Wei, Z.; Yang, J. H.; Zhou, J.; Xu, F.; Zrinyi, M.; Dussault, P. H.; Osada, Y.; Chen, Y. M. Self-healing gels based on constitutional dynamic chemistry and their potential applications. *Chem. Soc. Rev.* **2014**, *43*, 8114–8131.

(29) Li, Y.; Li, L.; Sun, J. Bioinspired Self-Healing Superhydrophobic Coatings. *Angew. Chem., Int. Ed.* **2010**, *49*, 6129–6133.

(30) White, S. R.; Sottos, N. R.; Geubelle, P. H.; Moore, J. S.; Kessler, M. R.; Sriram, S. R.; Brown, E. N.; Viswanathan, S. Autonomic healing of polymer composites. *Nature* **2001**, *409*, 794–797.

(31) Ghosh, B.; Urban, M. W. Self-Repairing Oxetane-Substituted Chitosan Polyurethane Networks. *Science* **2009**, *323*, 1458–1460.

(32) Capelot, M.; Montarnal, D.; Tournilhac, F.; Leibler, L. Metal-Catalyzed Transesterification for Healing and Assembling of Thermosets. *J. Am. Chem. Soc.* **2012**, *134*, 7664–7667.

(33) Ying, H.; Zhang, Y.; Cheng, J. Dynamic urea bond for the design of reversible and self-healing polymers. *Nat. Commun.* **2014**, *5*, 3218–3226.

(34) Cromwell, O. R.; Chung, J.; Guan, Z. Malleable and Self-Healing Covalent Polymer Networks through Tunable Dynamic Boronic Ester Bonds. *J. Am. Chem. Soc.* **2015**, *137*, 6492–6495.

(35) Kuhl, N.; Bode, S.; Bose, R. K.; Vitz, J.; Seifert, A.; Hoeppener, S.; Garcia, S. J.; Spange, S.; van der Zwaag, S.; Hager, M. D.; Schubert, U. S. Acylhydrazones as Reversible Covalent Crosslinkers for Self-Healing Polymers. *Adv. Funct. Mater.* **2015**, *25*, 3295–3301.

(36) Zhang, M. Q.; Rong, M. Z. Intrinsic self-healing of covalent polymers through bond reconnection towards strength restoration. *Polym. Chem.* **2013**, *4*, 4878–4884.

(37) Hart, L. R.; Harries, J. L.; Greenland, B. W.; Colquhoun, H. M.; Hayes, W. Healable supramolecular polymers. *Polym. Chem.* **2013**, *4*, 4860–4870.

(38) van Gemert, G. M. L.; Peeters, J. W.; Sontjens, S. H. M.; Janssen, H. M.; Bosman, A. W. Self-Healing Supramolecular Polymers In Action. *Macromol. Chem. Phys.* **2012**, *213*, 234–242.

(39) Chen, Y.; Kushner, A. M.; Williams, G. A.; Guan, Z. Multiphase design of autonomic self-healing thermoplastic elastomers. *Nat. Chem.* **2012**, *4*, 467–472.

(40) Hoogenboom, R. Hard Autonomous Self-Healing Supramolecular Materials-A Contradiction in Terms? *Angew. Chem., Int. Ed.* **2012**, *51*, 11942–11944.

(41) Yang, J. X.; Long, Y. Y.; Pan, L.; Men, Y. F.; Li, Y. S. Spontaneously Healable Thermoplastic Elastomers Achieved through One-Pot Living Ring-Opening Metathesis Copolymerization of Well-Designed Bulky Monomers. *ACS Appl. Mater. Interfaces* **2016**, *8*, 12445–12455.

(42) Wu, G.-P.; Daresbourg, D. J.; Lu, X. B. Tandem metal-coordination copolymerization and organocatalytic ring-opening polymerization via water to synthesize diblock copolymers of styrene oxide/ $\text{CO}_2$  and lactide. *J. Am. Chem. Soc.* **2012**, *134*, 17739–17745.

(43) Daresbourg, D. J.; Wu, G.-P. A one-pot synthesis of a triblock copolymer from propylene oxide/carbon dioxide and lactide: intermediacy of polyol initiators. *Angew. Chem., Int. Ed.* **2013**, *52*, 10602–10606.

(44) Wang, Y.; Fan, J. W.; Daresbourg, D. J. Construction of Versatile and Functional Nanostructures Derived from  $\text{CO}_2$ -based Polycarbonates. *Angew. Chem., Int. Ed.* **2015**, *54*, 10206–10210.

(45) Wu, G.-P.; Daresbourg, D. J. Mechanistic Insights into Water-Mediated Tandem Catalysis of Metal-Coordination  $\text{CO}_2$ /Epoxide Copolymerization and Organocatalytic Ring-Opening Polymerization: One-Pot, Two Steps, and Three Catalysis Cycles for Triblock Copolymers Synthesis. *Macromolecules* **2016**, *49*, 807–814.

(46) Yang, G.-W.; Wu, G.-P.; Chen, X. X.; Xiong, S. S.; Arges, C. G.; Ji, S. X.; Nealey, P. F.; Lu, X.-B.; Daresbourg, D. J.; Xu, Z.-K. Directed Self-Assembly of Polystyrene-b-poly(propylene carbonate) on Chemical Patterns via Thermal Annealing for Next Generation Lithography. *Nano Lett.* **2017**, *17*, 1233–1239.

(47) Wan, L. High  $\chi$  polystyrene-b-polycarbonate for next generation lithography. *Sci. China: Chem.* **2017**, *60*, 679–680.

(48) Kember, M. R.; Copley, J.; Buchard, A.; Williams, C. K. Triblock copolymers from lactide and telechelic poly(cyclohexene carbonate). *Polym. Chem.* **2012**, *3*, 1196–1201.

(49) Kember, M. R.; Williams, C. K. Adding Value to Power Station Captured  $\text{CO}_2$ : Tolerant Zn and Mg Homogeneous Catalysts for Polycarbonate Polyol Production. *J. Am. Chem. Soc.* **2012**, *134*, 15676–15679.

(50) Łukaszczuk, J.; Jaszcz, K.; Kuran, W.; Listoś, T. Synthesis and modification of functional polycarbonates with pendant allyl groups. *Macromol. Biosci.* **2001**, *1*, 282–289.

(51) Tan, C.-S.; Kuo, T.-W. Synthesis of polycarbonate-silica nanocomposites from copolymerization of  $\text{CO}_2$  with allyl glycidyl ether, cyclohexene oxide, and sol-gel. *J. Appl. Polym. Sci.* **2005**, *98*, 750–757.

(52) Tao, Y.; Wang, X.; Zhao, X.; Li, J.; Wang, F. Crosslinkable poly(propylene carbonate): High-yield synthesis and performance improvement. *J. Polym. Sci., Part A: Polym. Chem.* **2006**, *44*, 5329–5336.

(53) Daresbourg, D. J.; Wang, Y. Terpolymerization of propylene oxide and vinyl oxides with  $\text{CO}_2$ : copolymer cross-linking and surface modification via thiol–ene click chemistry. *Polym. Chem.* **2015**, *6*, 1768–1776.

(54) Subhani, M. A.; Kohler, B.; Gütler, C.; Leitner, W.; Müller, T. E. Transparent Films from  $\text{CO}_2$ -Based Polyunsaturated Poly(ether carbonate)s: A Novel Synthesis Strategy and Fast Curing. *Angew. Chem., Int. Ed.* **2016**, *55*, 5591–5596.

(55) Deng, K.; Wang, S.; Ren, S.; Han, D.; Xiao, M.; Meng, Y. A Novel Single-Ion-Conducting Polymer Electrolyte Derived from  $\text{CO}_2$ -Based Multifunctional Polycarbonate. *ACS Appl. Mater. Interfaces* **2016**, *8*, 33642–33648.